



TALE実験ハイブリッド観測による エネルギースペクトル測定

大島 仁 for the TA Collaboration
ICRR, the University of Tokyo
oshima@icrr.u-tokyo.ac.jp

第七回 空気シャワー観測による宇宙線の起源探索研究会,
東京大学宇宙線研究所, Mar. 25 – 27, 2024

Introduction

TALE (10^{15} - 10^{18} eV) & TA, TAx4 ($> 10^{18}$ eV) can cover a wide-energy range of 5 orders of magnitude from 10^{15} eV to 10^{20} eV.

Acceleration limit of galactic CRs
beginning of extragalactic CRs

Shielding and confinement of galactic CRs

Structure of the GMF and EGMF

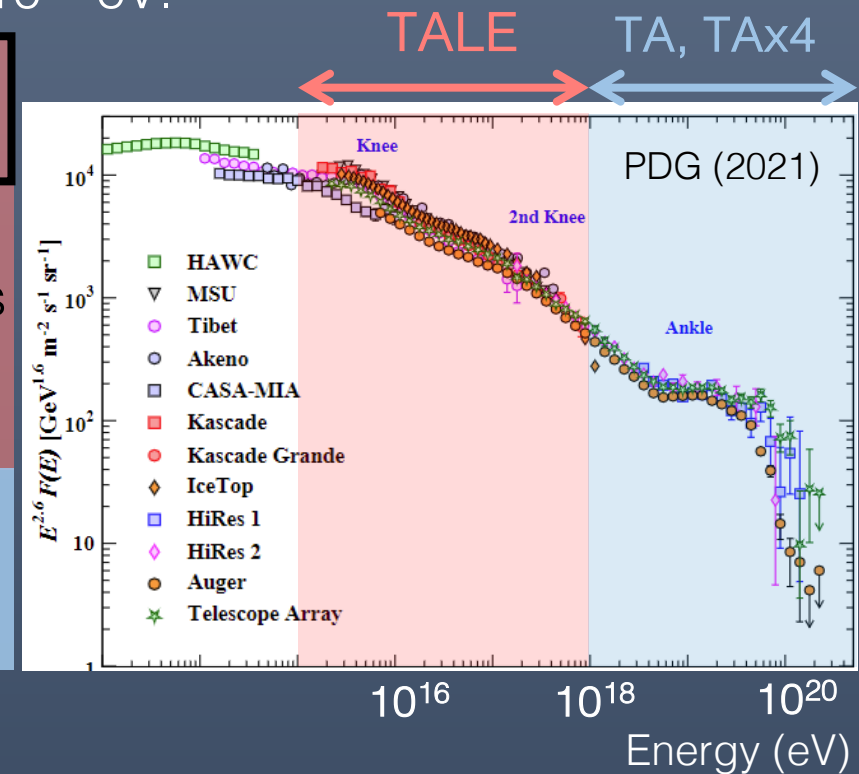
Origins of the extra galactic cosmic rays

The energy spectrum reflects these physical phenomena in complex.

As the first physical goal, through the measurements of

- Composition and energy spectrum, and
- Transition from galactic to extragalactic cosmic rays,

we aim to measure the acceleration limit of galactic cosmic rays.



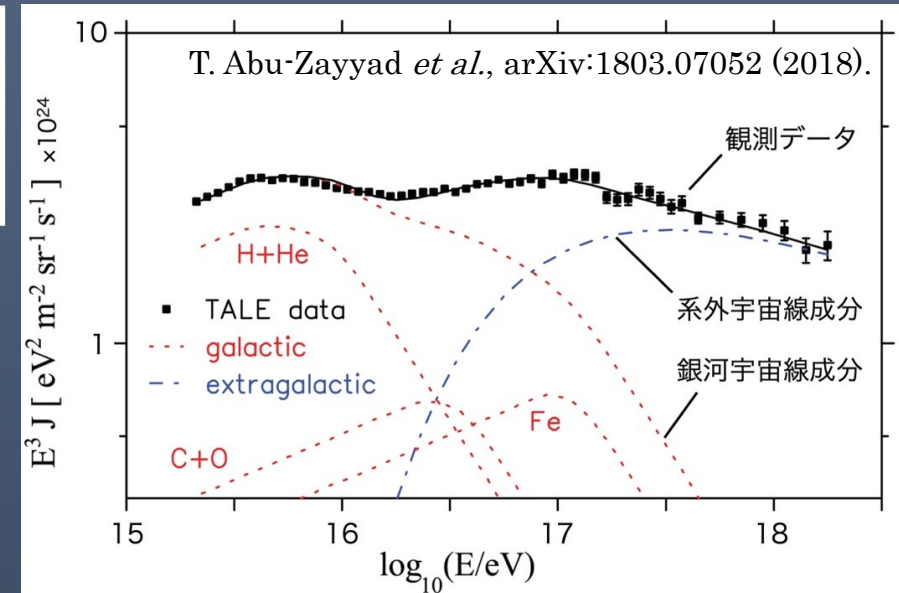
Introduction (Cont'd)

How do we approach the acceleration limit of galactic CRs?
beginning of extragalactic CRs?

Strategy:
Energy spectrum + Composition

Separate the energy spectra
of galactic and extragalactic
CRs

As the first step, we measured the
inclusive energy spectrum from
 $10^{16.5}$ eV to $10^{18.1}$ eV with the TALE
hybrid mode.

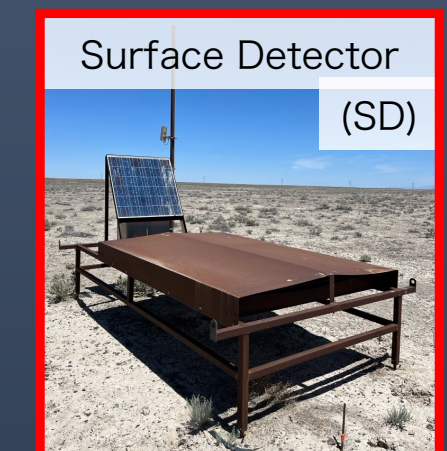
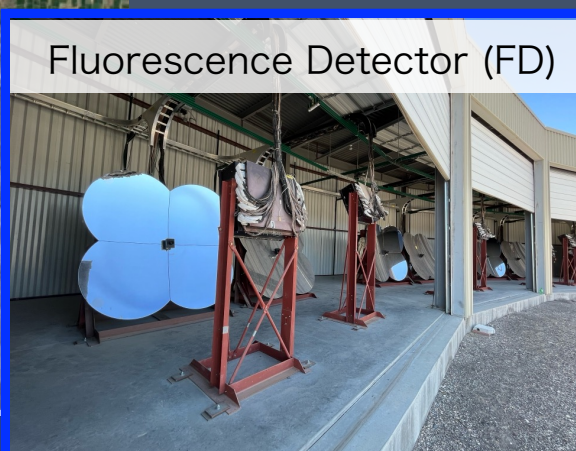
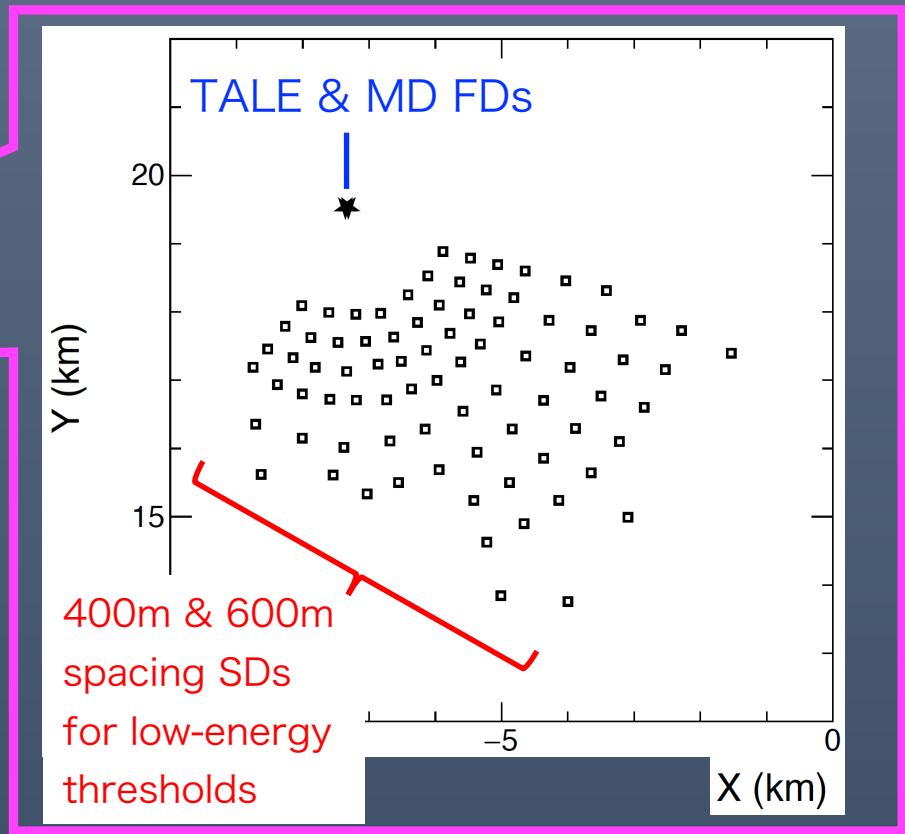
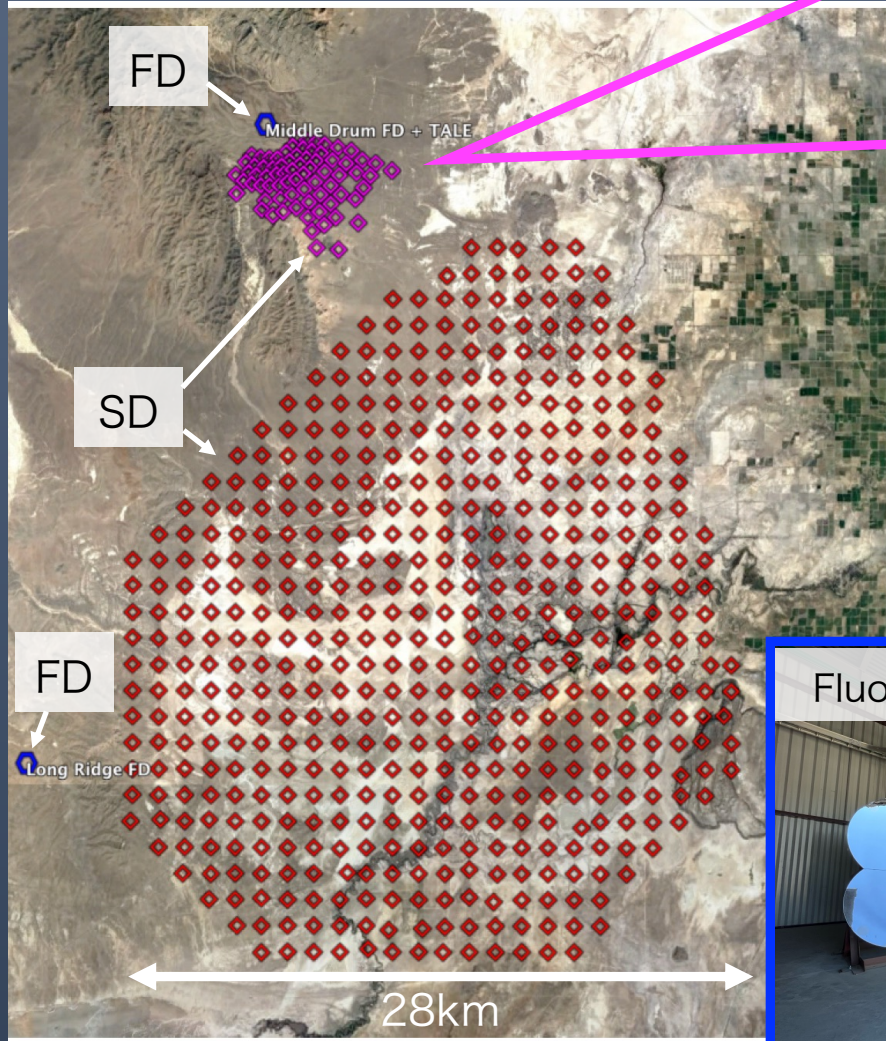


Galactic cosmic rays:
Proton → Iron

Extragalactic cosmic rays:
Proton (or heavier nucleus?)
3

Physical location of the TALE detector

The TA & TALE detectors are located in Millard County, Utah, USA.

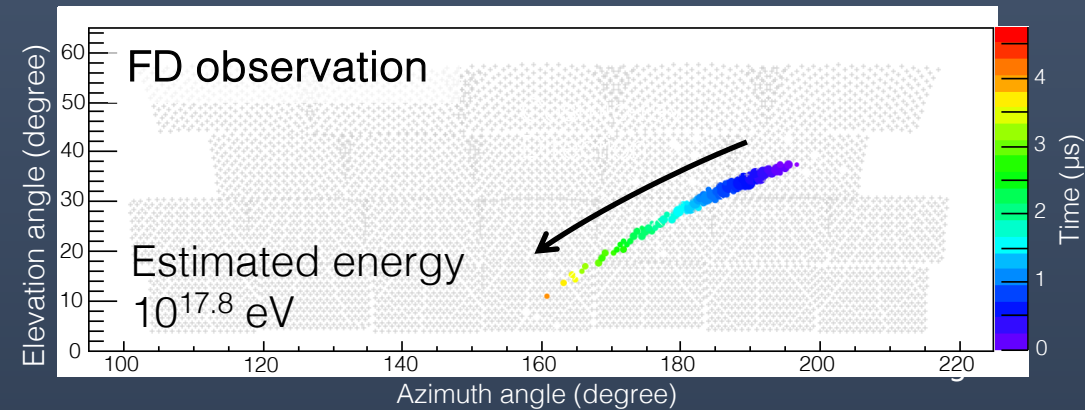
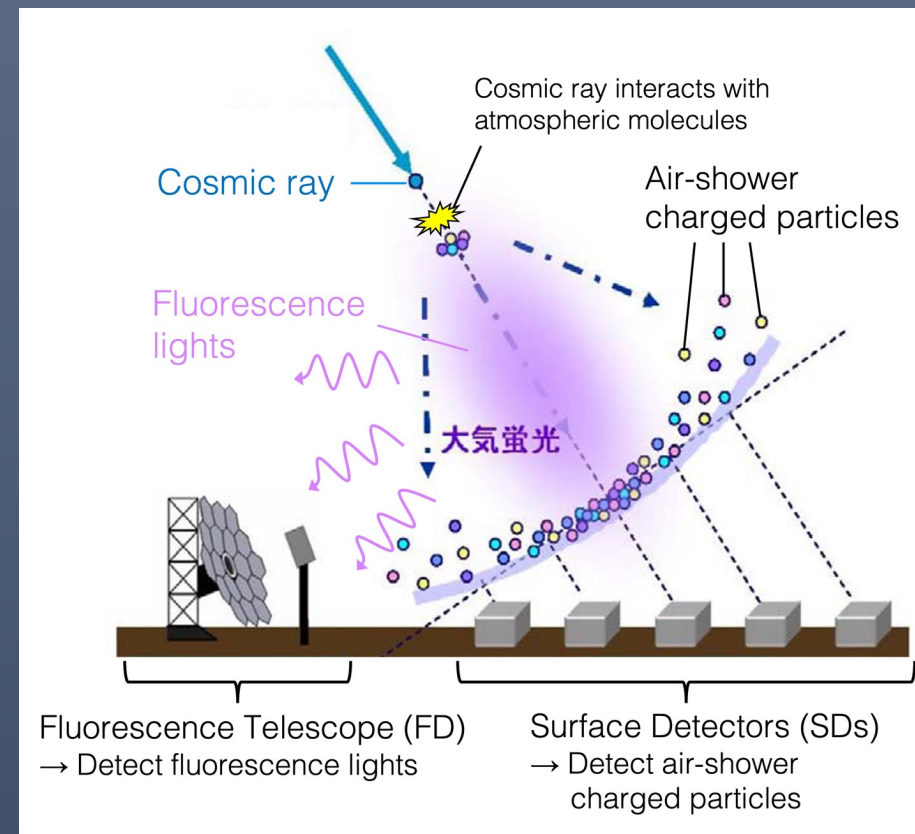
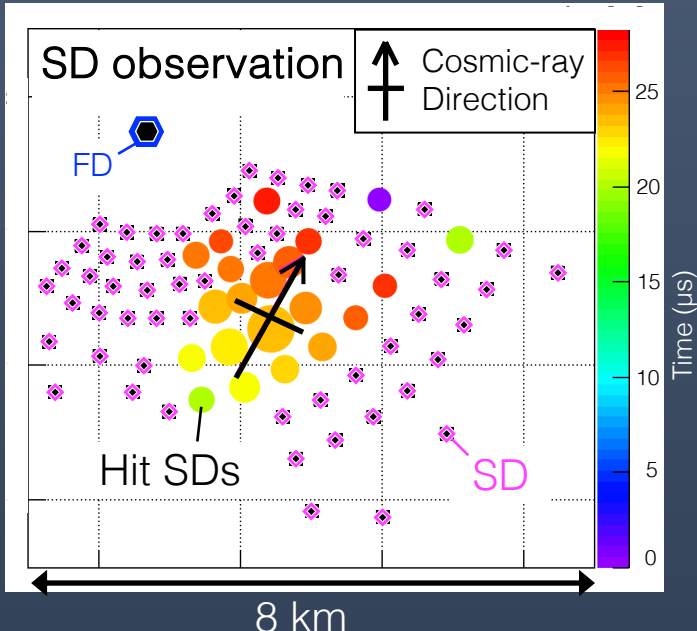


Analysis strategy: Hybrid analysis

Hybrid analysis using FD and SD array

- X_{\max} measurement
→ Composition sensitive
- Energy resolution is improved using SD array for shower-axis detection.

Event displays of the SD array and the FD.



Monte Carlo Simulation

Monte Carlo (MC) simulation is performed following processes:

(1) Air-Shower simulation (CORSIKA)

- Hadronic interaction model: QGSJETII-04, Proton and Iron
- Energy range: $16.2 \leq \log E \leq 18.5$

“Reuse” events with random distributions in core position and azimuth angle.

(2) SD simulation

- The energy deposit in each SD with Geant4
- Detector calibration using the monitor data
- Response of the SD electronics

(3) FD simulation

- Fluorescence and Cherenkov photons are generated.
- Telescope optics and detector calibration are taken into account.

(4) Hybrid analysis simulation

- Same processes for the data analysis are performed.

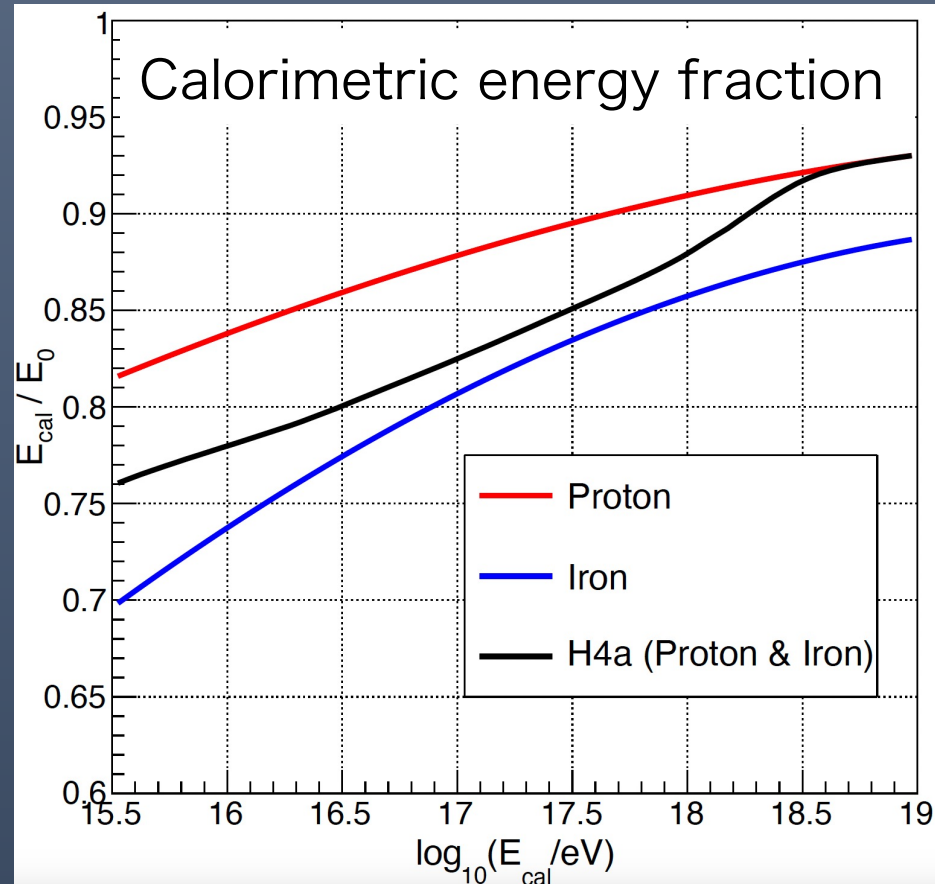
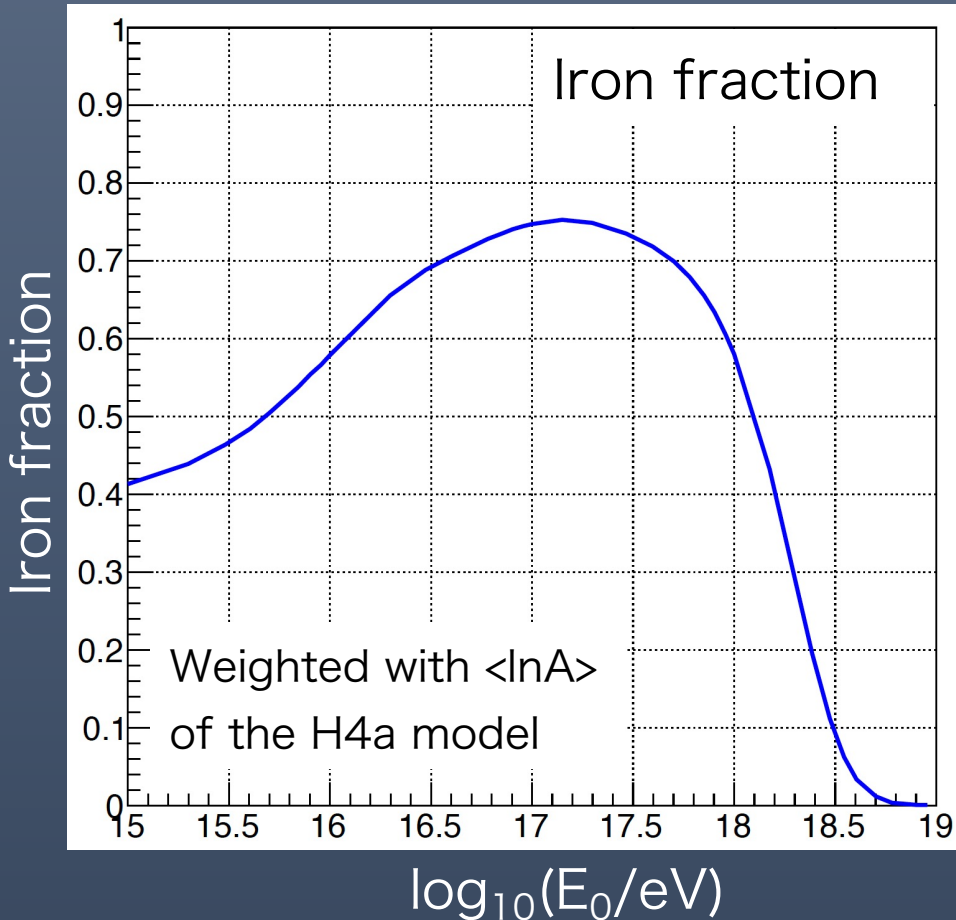
Event selection

Hybrid trigger events: FD + any1 SD w/ 1 MIP

Events with a fractional contribution to the total signal of fluorescence light less than 75% are defined as CL events, while the others are defined as FL events.

	CL	FL
No Cut	Hybrid triggered events	
Selection 1	No saturated PMTs in TALE-FD	
Selection 2	Sel.1 + X_{\max} is inside the geometrical field of view of the FDs $+ 210 \text{ g/cm}^2 < X_{\max} + \chi^2_{\text{long}} / \text{ndf} < 100$	
Selection 3	-	Sel.2 + # of photo-electrons > 2000
Selection 4	Sel.3 + Event duration > 100 ns	-
Selection 5	Sel.4 + # of PMTs > 10	-
Selection 6	Sel.5 + # of photo-electrons/# of PMTs > 50	-
Selection 7	Sel.6 + Angular track length > 6.5 deg	-
Selection 8	Sel.7 + $\log(E_{\text{rec}} / \text{eV}) > 16.5 + \theta_{\text{zenith}} < 60^\circ$	
Selection 9	Good weather	

Iron fraction and missing energy correction on H4a composition model

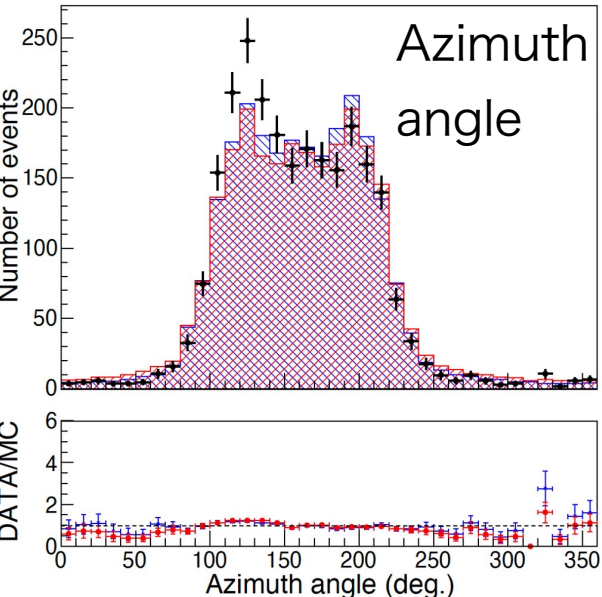
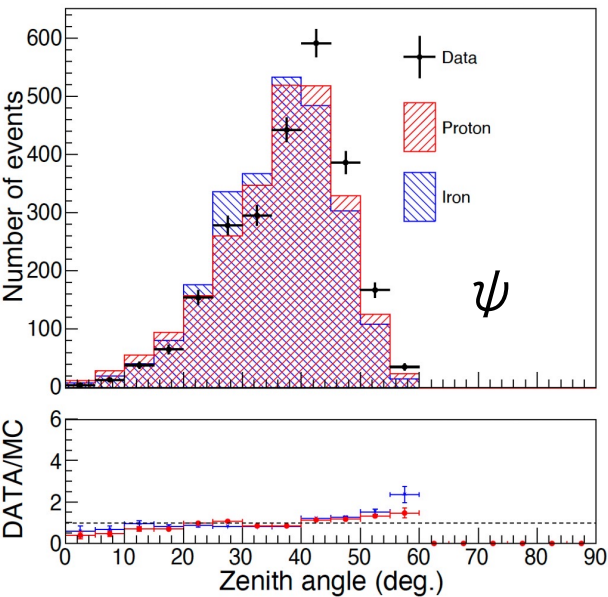
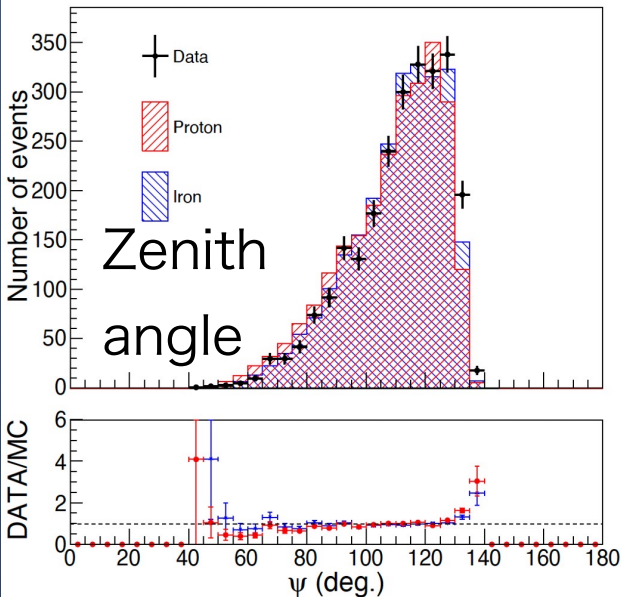
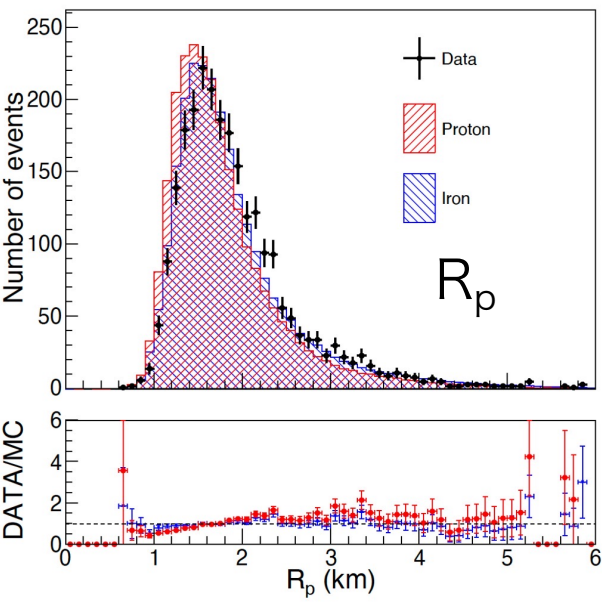
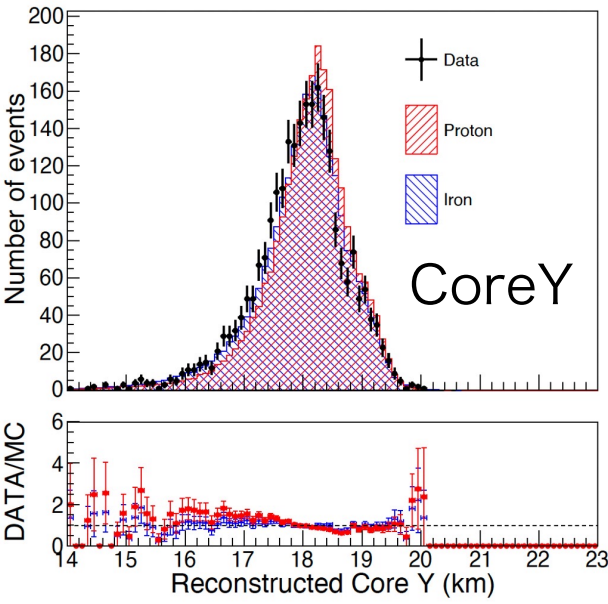
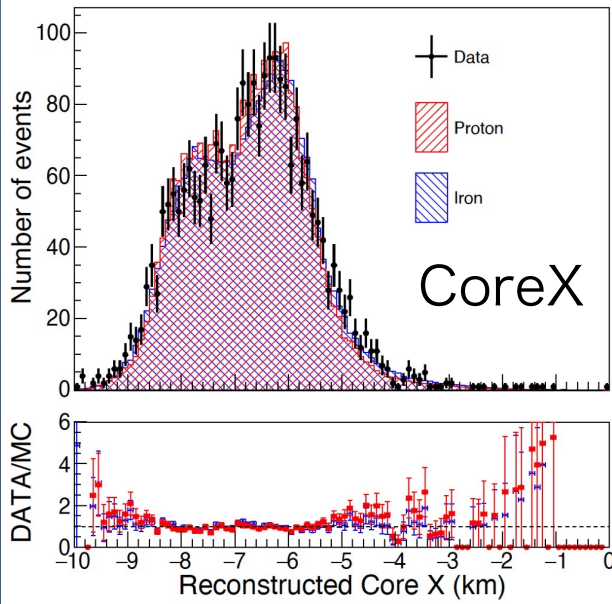


We assumed proton and iron compositions using H4a model.
We are also preparing the MC data set of helium and nitrogen now.

Comparison between the data & MC prediction

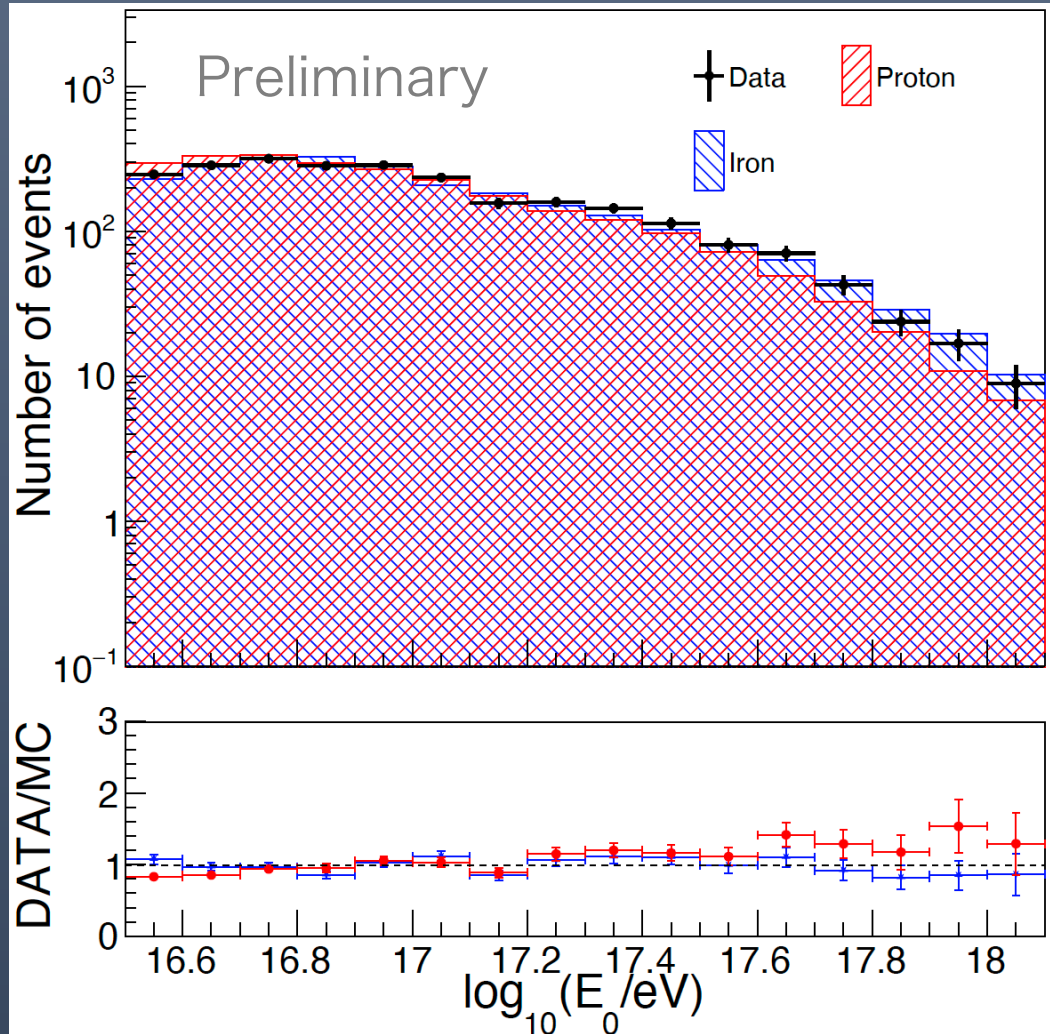
Preliminary

Points: Data, Histograms: MC (Area normalized)

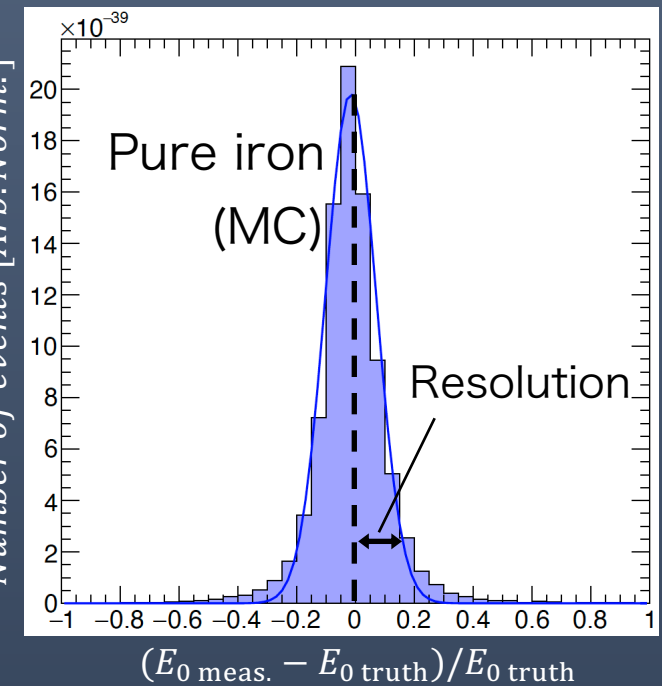


Energy measurements

Points: Data, Histogram: MC (Area normalized)



Energy Resolution (MC)
Pure proton : 10.1%
Pure iron : 8.6%



Measured energy is consistent with the MC prediction.

Energy resolution is consistent with previous studies.

Iterative D'Agostini unfolding

The Iterative unfolding uses Bayes' theorem to obtain an unsmeared matrix from the smearing matrix.

$$\text{Unfolded spectrum} \rightarrow C'_i = \sum_{j=1}^{N_m} U_{ij} E_j^{\text{data}}$$

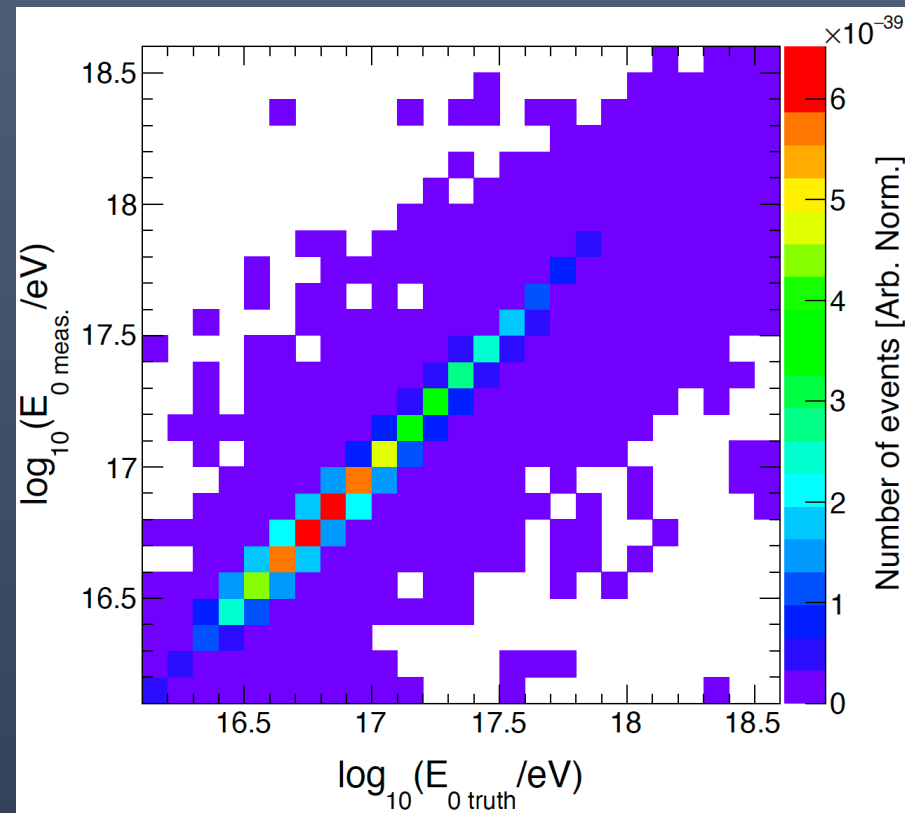
Smearing matrix

Number of events in measured bin j

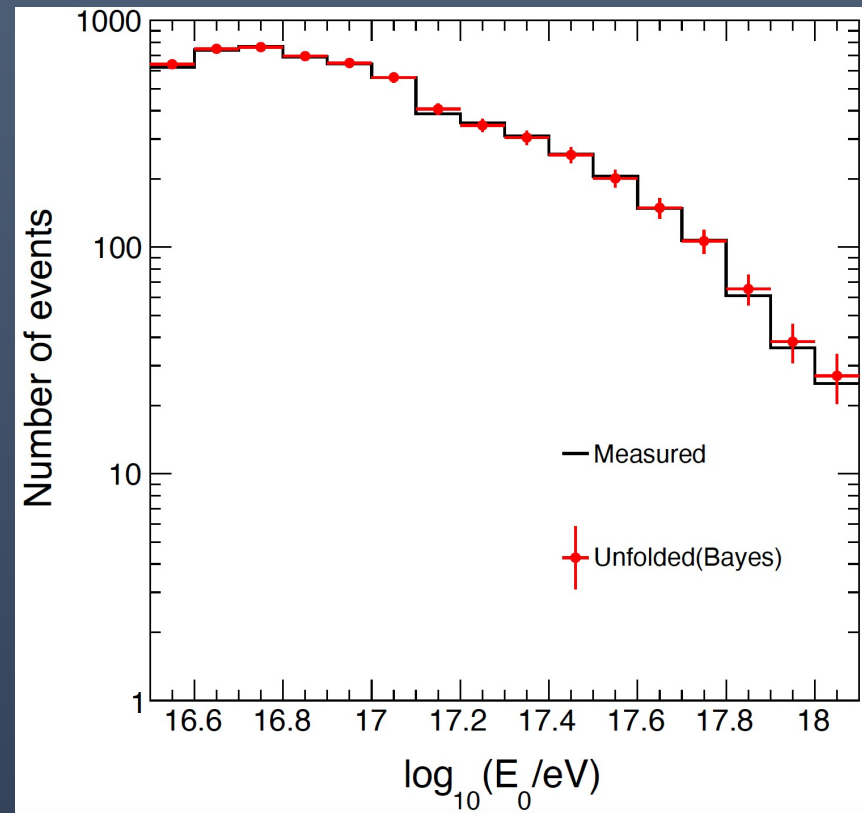
G. D'Agostini, arXiv:1010.0632.

G. D'Agostini, Nucl. Instrum. Methods Phys. Res., Sect A **362**, 487 (1995).

Resolution map of energy measurement



Energy distributions (Data)



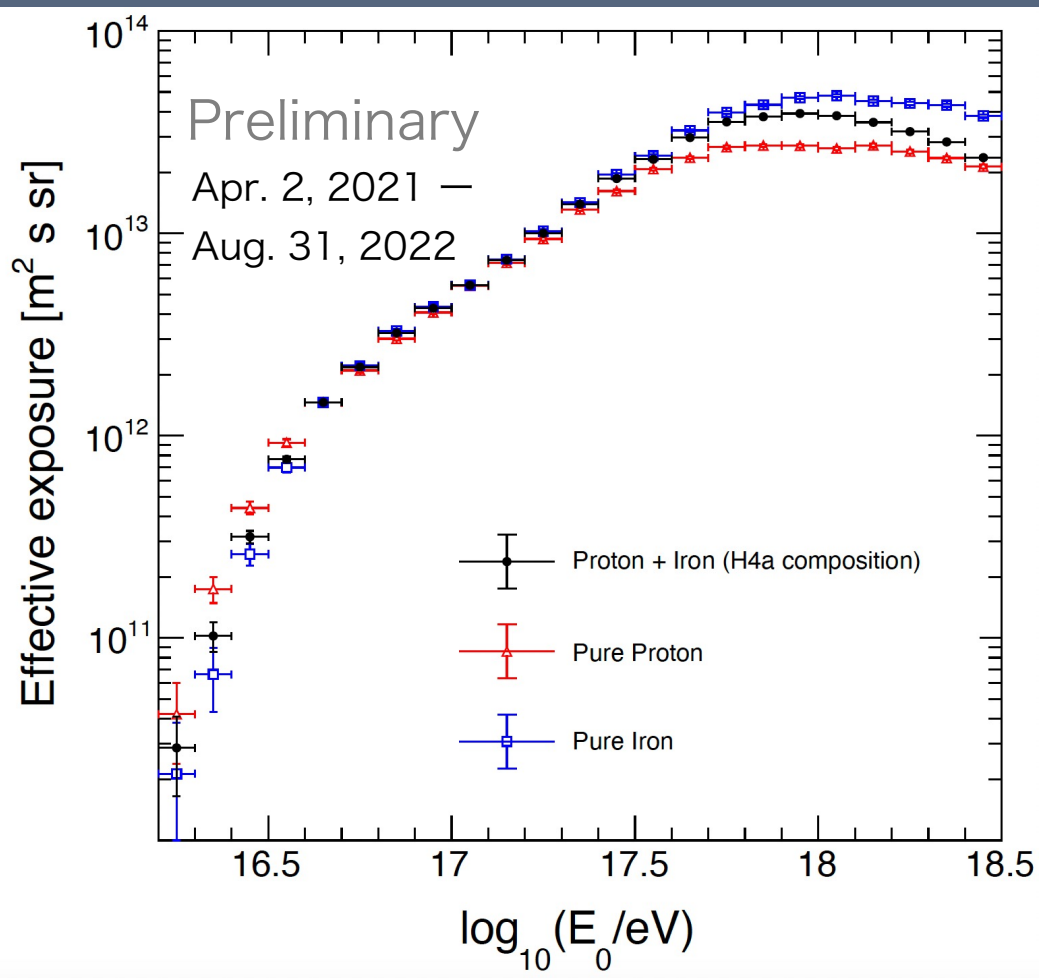
Equation of energy spectrum

$$J(E_i) = \frac{\sum_{j=1}^{N_m} U_{ij} N_j^{\text{sel}}}{A\Omega(E_i) \cdot T \cdot \Delta E_i}$$

Number of events with unfolding
Effective exposure for the true energy spectrum

- $J(E_i)$: Differential Flux [$\text{m}^2 \cdot \text{s}^{-1} \cdot \text{sr}^{-1} \cdot \text{eV}^{-1}$]
- U_{ij} : Unsmearing matrix
- N_j^{sel} : Number of selected events
- $A\Omega(E_i)$: Effective aperture [$\text{m}^2 \cdot \text{sr}$]
- T : Observation time [s]
- ΔE_i : Width of i-th bin

Effective Exposure



Effective exposure is evaluated using the MC simulation.

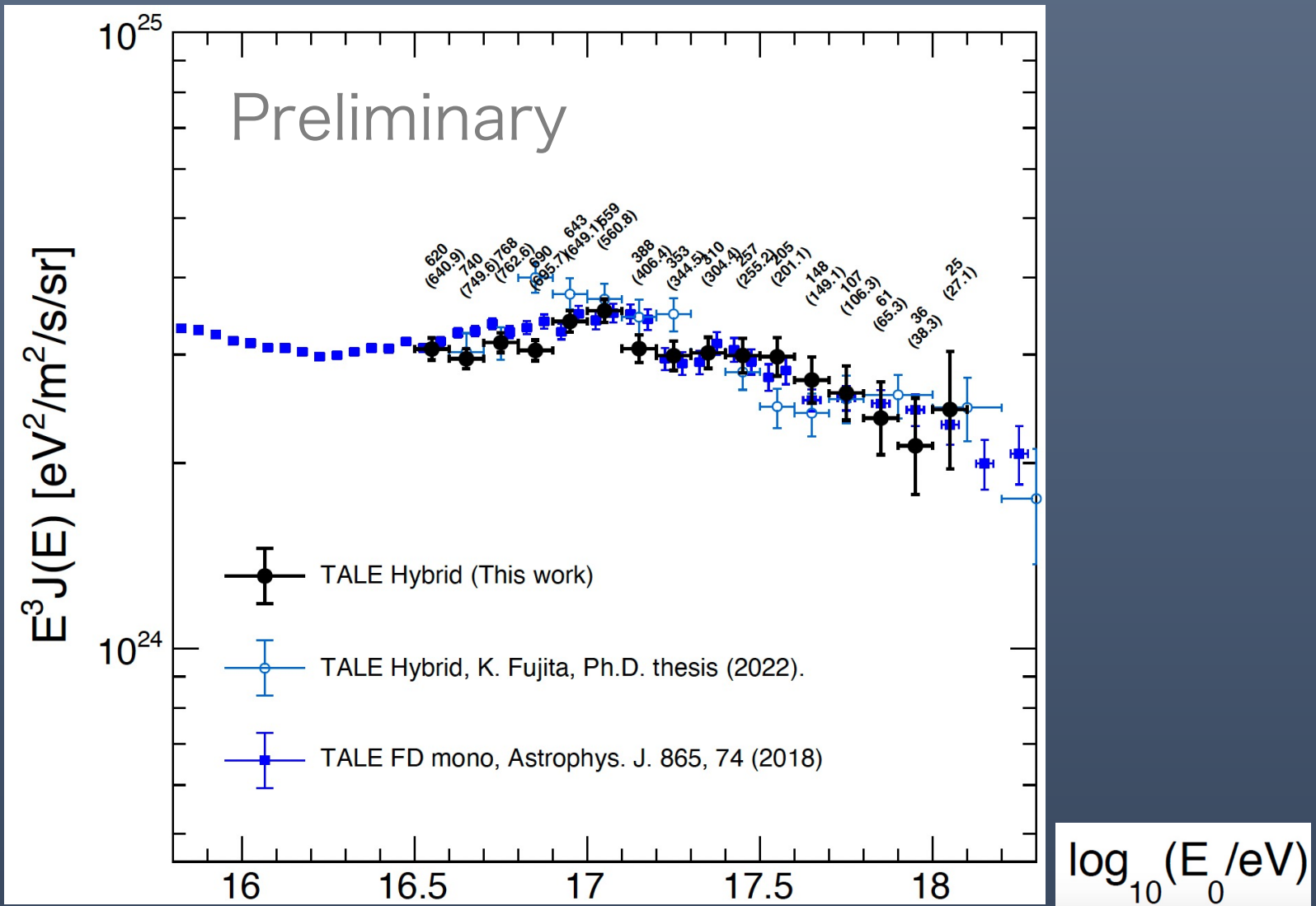
Geometrical aperture : **299.8 km² · sr**

- Area : 127.2 km²
- Zenith angle : $\theta_{\text{zenith}} < 60^\circ$

Observation time : 910 hours

Nov. 14, 2018 – Feb. 29, 2020: 369 hours
Apr. 2, 2021 – Aug. 31, 2022: 541 hours

Results: Energy spectrum

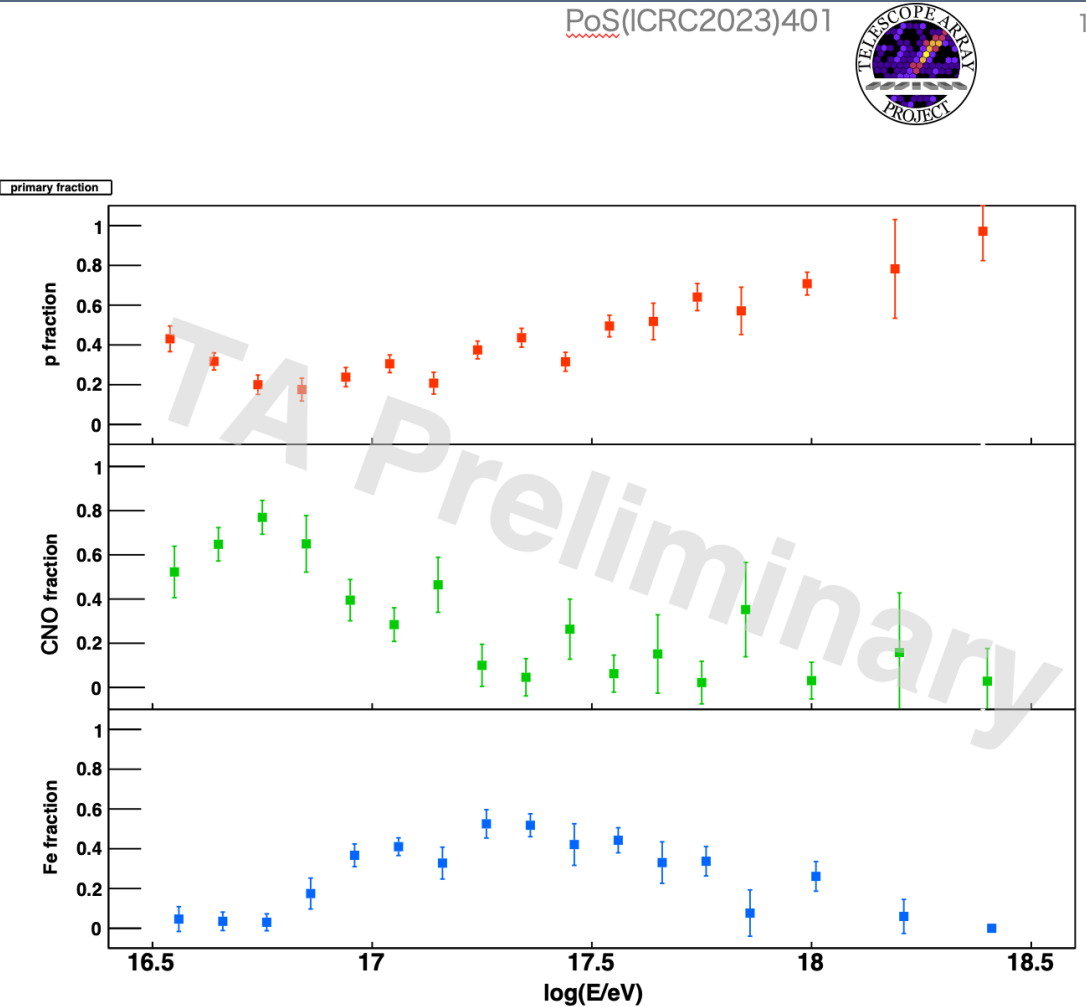


MC studies with other hadronic interaction model and compositions is ongoing.

Composition

Fraction of UHECR primaries

- proton
 - lowest fraction ~ 100 PeV
 - continue climb up to 3 EeV
- CNO
 - peak at ~ 50 PeV
 - low contribution in $E > 1$ EeV
- iron
 - peak at ~ 150 PeV \sim 2nd knee
 - roughly 26/7x higher energy than CNO



2023/09/17

「宇宙線で繋ぐ文明・地球環境・太陽系・銀河」

Combine with the energy spectrum \rightarrow each composition spectrum
 \rightarrow Information for the galactic- and extragalactic- energy spectra

Summary & Prospects

- Aim of the TALE hybrid analysis:

Using spectrum and composition measurements in 10^{16} eV– 10^{18} eV

- Measure the acceleration limit of galactic cosmic rays
- Separate galactic and extragalactic components

- Using the 910 hours observation data of the TALE hybrid detector

- Data/MC comparison of the fundamental parameters
 - Measurement of the energy distribution
- The data are generally reproduced by the MC simulation

- We measured the energy spectrum and the composition

- Energy spectra of each composition
- Information for the galactic- and extragalactic- energy spectra

Discussion

- TALE + TAの広エネルギー範囲の宇宙線観測データはもっと有効活用できるはず。
- 少なくともTALEのデータをハドロン相互作用モデルの検証に使用できるはず。
 - どんなデータを
 - どのように使えるか。
使えるか。
- 他の物理に対しては？



Thank you for your attention!



TALE infill array deployment
Nov 15, 2022.

Backup

Resolution of energy measurement

TALE FD mono obs.

	Energy Resolution
Cherenkov dominant (All energy)	15.9%
Cherenkov dominant ($E > 10^{16.7}$ eV)	8.7%
Fluorescence dominant	10.3%

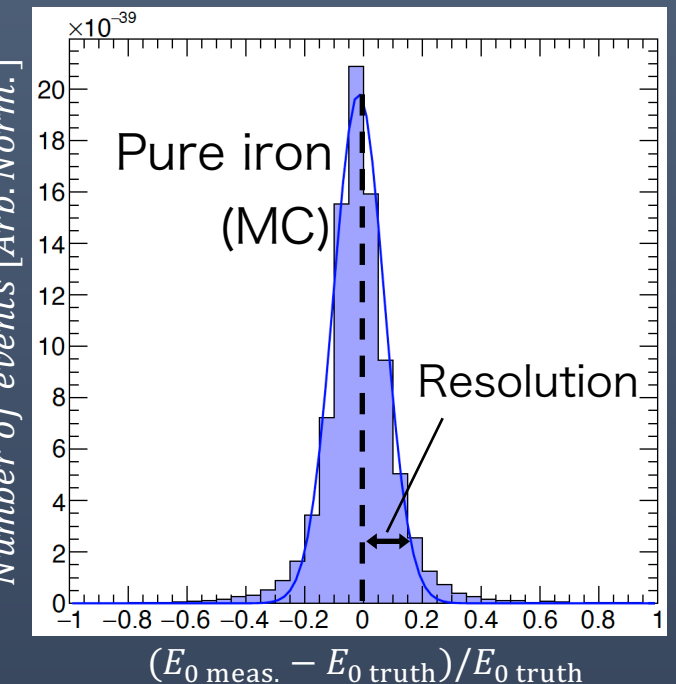
TALE Hybrid obs.

	Energy Resolution
Pure proton	10.1%
Pure iron	8.6%

TALE Hybrid
Resolution (MC)

Pure proton : 10.1%

Pure iron : 8.6%



Resolution of Xmax measurement

TALE FD mono obs.

	Xmax Resolution
Cherenkov dominant (All energy)	46.43 g/cm ²
Cherenkov dominant ($E > 10^{16.7}$ eV)	35.93 g/cm ²
Fluorescence dominant	58.87 g/cm ²

R. U. Abbashi et al., *Astrophys. J.* **865**, 74 (2018).

TALE Hybrid obs.

	Xmax Resolution
Pure proton	29.1 g/cm ²
Pure iron	26.6 g/cm ²

K. Fujita, Ph.D. thesis (2022).

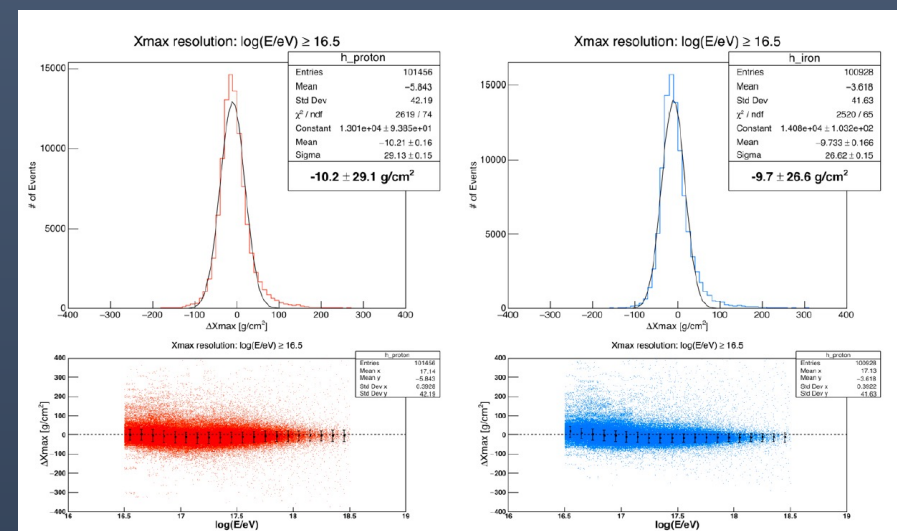
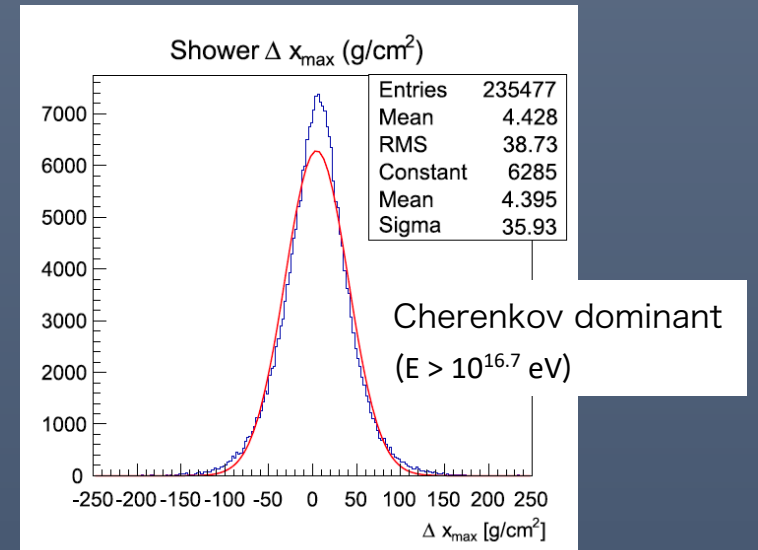


FIGURE 4.23: TALE Hybrid X_{max} angle reconstruction resolution histograms by evaluating $(X_{\text{max}} \text{ recon} - X_{\text{max}} \text{ thrown})$.

Spectrum index for MC weights

Table 6

Fit Parameters to a Broken Power-law Fit to the TALE Spectrum

$\log_{10}(E_1)$	$16.22 \pm 0.017 \pm 0.10$
$\log_{10}(E_2)$	$17.04 \pm 0.035 \pm 0.09$
$\gamma_1: 15.70 < \log_{10}(E) < 16.22$	$3.12 \pm 0.007 \pm 0.043$
$\gamma_2: 16.22 < \log_{10}(E) < 17.04$	$2.92 \pm 0.008 \pm 0.012$
$\gamma_3: 17.04 < \log_{10}(E) < 18.30$	$3.19 \pm 0.017 \pm 0.026$

R. U. Abbashi et al., *Astrophys. J.*, **865**, 74 (2018).

	γ_3	$\log_{10}(E/\text{eV})$	γ_4
HiRes	-3.25 ± 0.01	18.65 ± 0.05	-2.81 ± 0.03

	γ_4	$\log_{10}(E/\text{eV})$	γ_5
HiRes	-2.81 ± 0.03	19.75 ± 0.05	-5.1 ± 0.7

R. U. Abbashi et al., *Phys. Rev. Lett.* **100**, 101101 (2008).

Energy region	γ
$\log_{10}(E/\text{eV}) < 16.22$	-3.12 ± 0.044
$16.22 \leq \log_{10}(E/\text{eV}) < 17.04$	-2.92 ± 0.014
$17.04 \leq \log_{10}(E/\text{eV}) < 18.65$	-3.19 ± 0.031
$18.65 \leq \log_{10}(E/\text{eV}) < 19.75$	-2.81 ± 0.03
$19.75 \leq \log_{10}(E/\text{eV})$	-5.1 ± 0.7

TALE Hybrid Spectrum with TA result

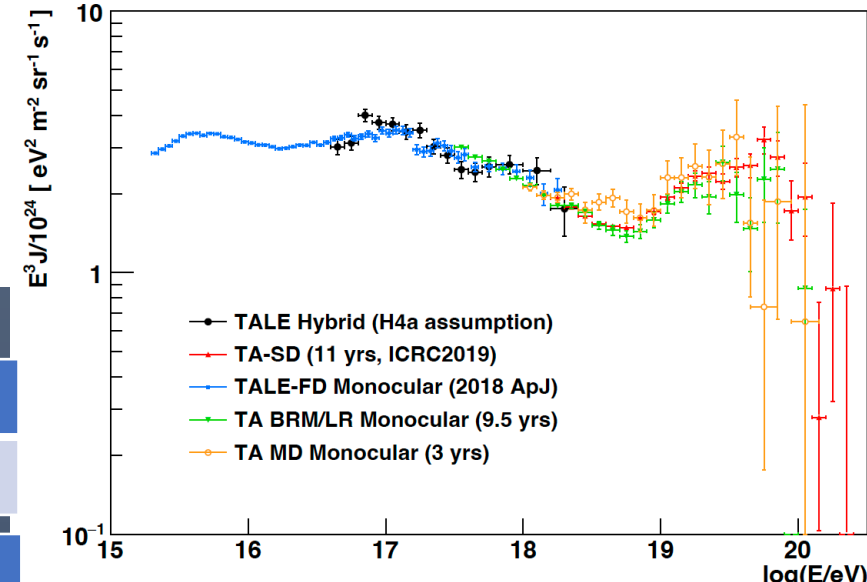


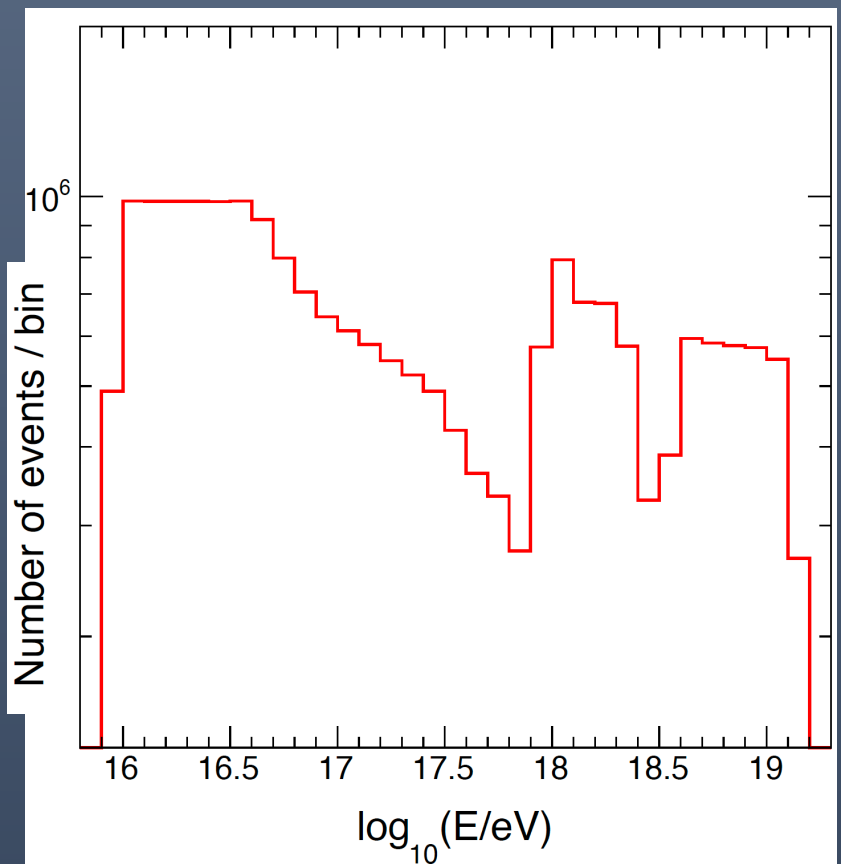
FIGURE 5.33: TALE hybrid cosmic ray energy spectrum comparison with measurements by the TALE FD monocular mode [26], by the TA using the FDs at Black Rock Mesa, Long Ridge [96] and Middle Drum [97] sites, and by the TA SD [25].

K. Fujita, Ph. D. thesis (2022).

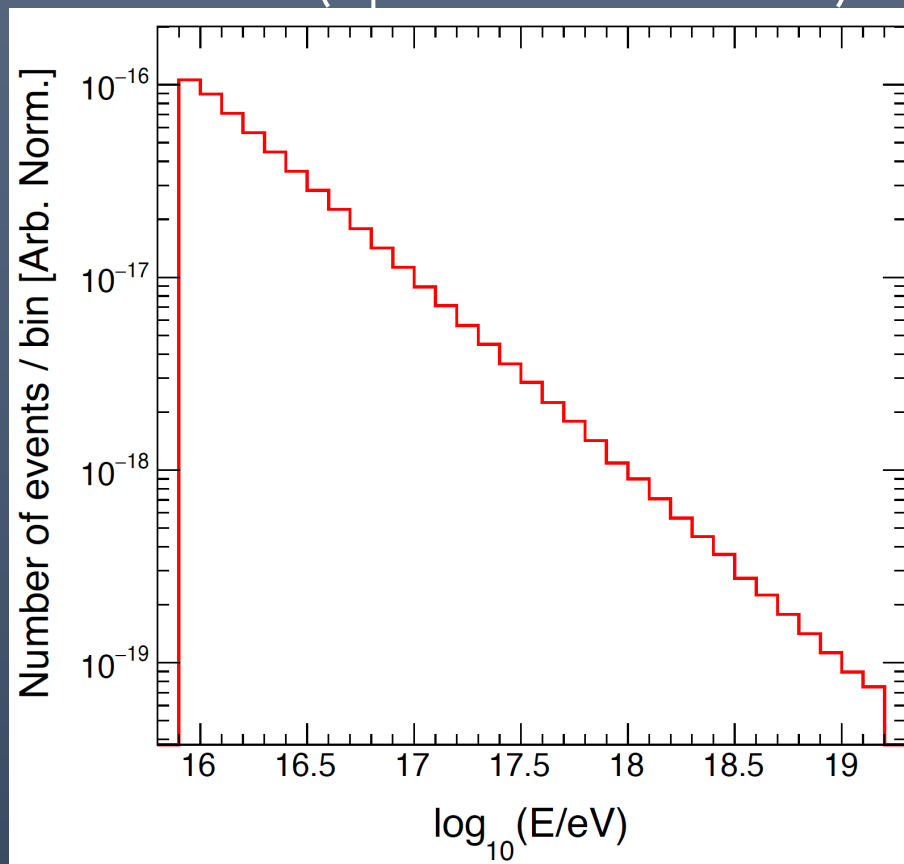
These spectrum indexes are used for a weighting factor of the MC predictions.

Energy spectrum : Thrown to spectral index of -2

Thrown



Thrown (Spectral index of 2)



$$N_{i-\text{th}} \times (E^{-1} / N_{i-\text{th}})$$

Energy spectrum : Weight for spectrum index of -2

$$W(E) = E^2 \log_{10} E \times f_{\text{spectrum}}$$

$$\log_{10}(E/\text{eV}) < 16.22 : f_{\text{spectrum}} = 10^{\gamma_1 \log E}$$

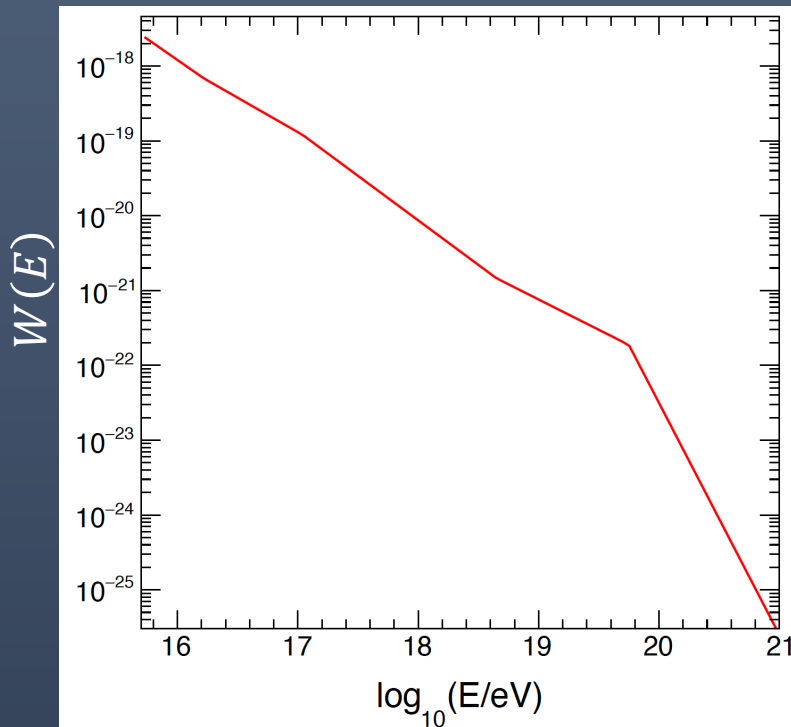
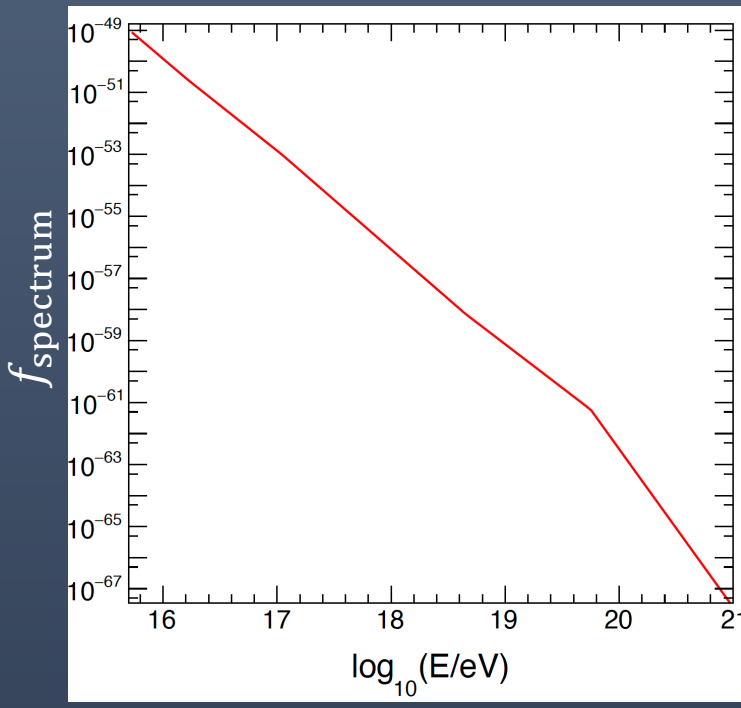
$$16.22 \leq \log_{10}(E/\text{eV}) < 17.04 : f_{\text{spectrum}} = 10^{(\gamma_1 - \gamma_2) \times \log E} \times 10^{\gamma_2 \times \log E}$$

$$17.04 \leq \log_{10}(E/\text{eV}) < 18.65 : f_{\text{spectrum}} = 10^{(\gamma_1 - \gamma_2) \times \log E} \times 10^{(\gamma_2 - \gamma_3) \times \log E} \times 10^{\gamma_3 \times \log E}$$

$$18.65 \leq \log_{10}(E/\text{eV}) < 19.75 : f_{\text{spectrum}} = 10^{(\gamma_1 - \gamma_2) \times \log E} \times 10^{(\gamma_2 - \gamma_3) \times \log E} \times 10^{(\gamma_3 - \gamma_4) \times \log E} \times 10^{\gamma_4 \times \log E}$$

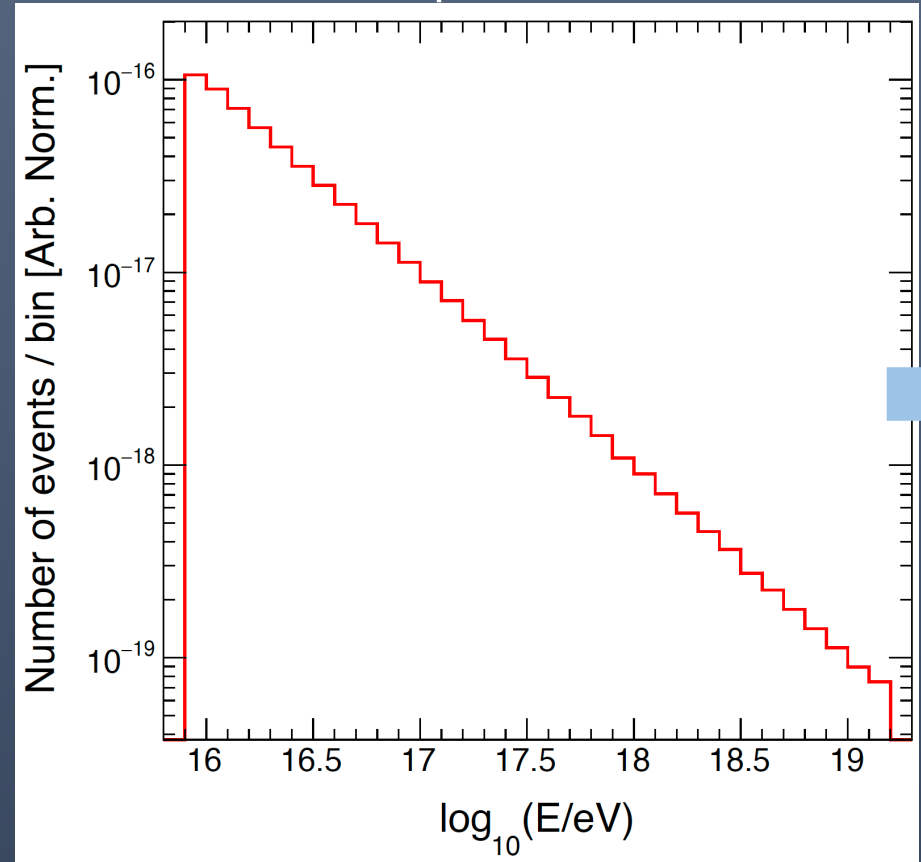
$$19.75 \leq \log_{10}(E/\text{eV}) : f_{\text{spectrum}} = 10^{(\gamma_1 - \gamma_2) \times \log E} \times 10^{(\gamma_2 - \gamma_3) \times \log E} \times 10^{(\gamma_3 - \gamma_4) \times \log E} \times 10^{(\gamma_4 - \gamma_5) \times \log E} \times 10^{\gamma_5 \times \log E}$$

γ	Value
γ_1	-3.12
γ_2	-2.92
γ_3	-3.19
γ_4	-2.81
γ_5	-5.1

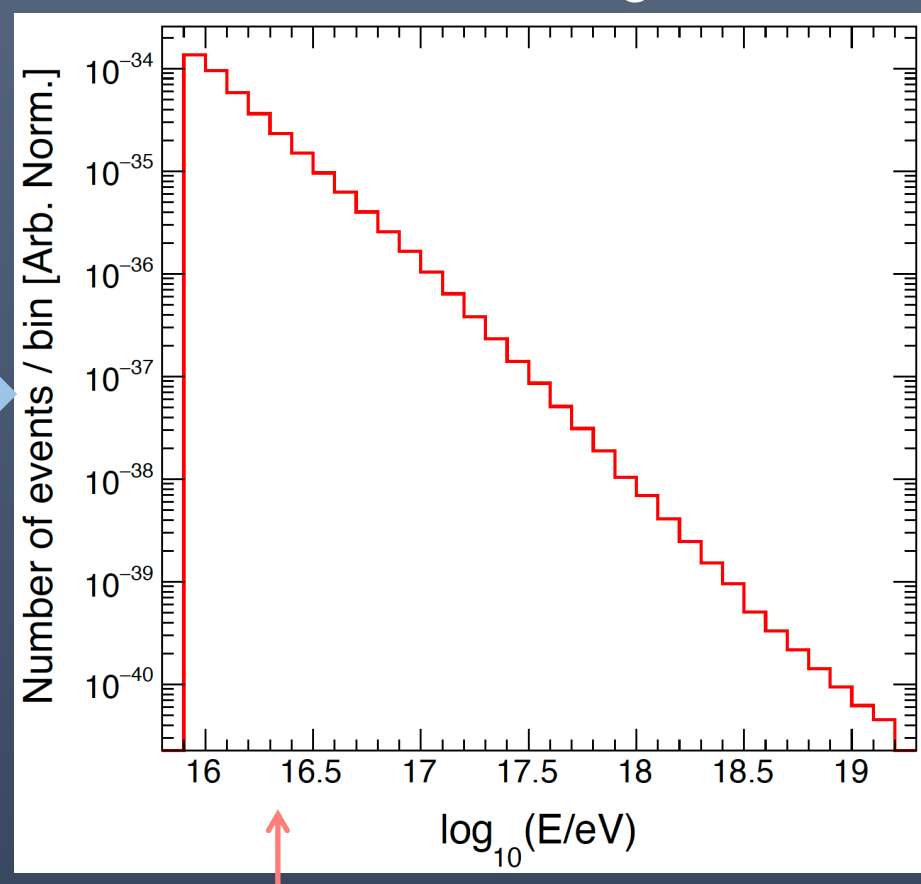


Energy spectrum : spectral index of -2 to weighted

Thrown (Spectral index of 2)



Thrown (Weighted)



$$N_{i-\text{th}} \times (E^{-1}/N_{i-\text{th}}) \times W(E)$$

MC events are weighted
using this histogram.²⁵

Iterative D'Agostini unfolding

The Iterative unfolding uses Bayes' theorem to obtain an unsmeared matrix from the smearing matrix.

$$\text{Unfolded spectrum} \rightarrow C'_i = \sum_{j=1}^{N_m} U_{ij} E_j^{\text{data}}$$

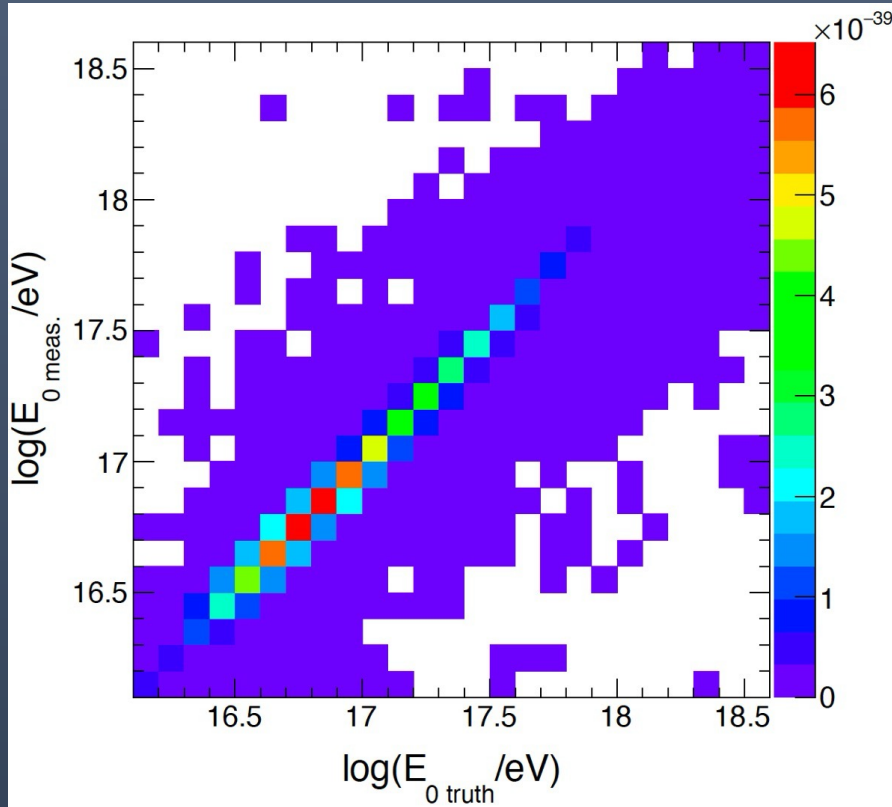
Smearing matrix

Number of events in measured bin j

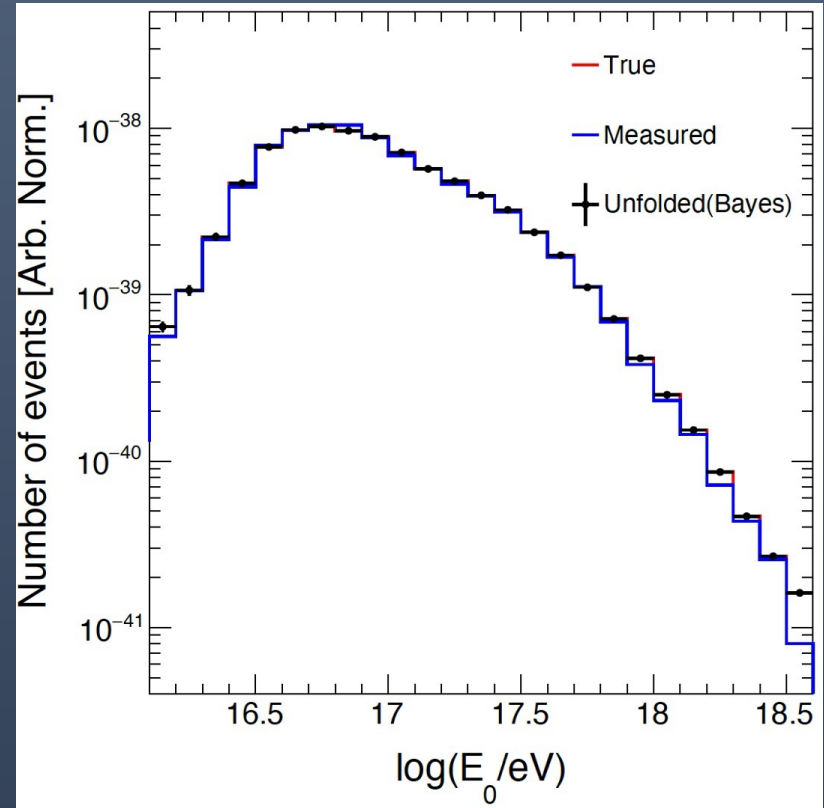
G. D'Agostini, arXiv:1010.0632.

G. D'Agostini, Nucl. Instrum. Methods Phys. Res., Sect A **362**, 487 (1995).

Resolution map of energy measurement



Energy distribution w/ unfolding (MC)



Iterative D'Agostini unfolding (1)

The relation between true and measured spectrum is written by

$$E_j = \sum_{i=1}^{N_t} S_{ji} C_i,$$

where C_i is a number of events in true bin i , E_i is a number of events in measured bin j , S_{ji} is a smearing matrix, and N_t is the number true bins.

An unsmearing matrix can be obtained from the smearing matrix as

$$U_{ij} = \frac{P_{eff}(E_j|C_i)P_0(C_i)}{\sum_{i=1}^{N_t} P(E_j|C_i)P_0(C_i)},$$

where $P(E_j|C_i)$ is a probability of the true events in bin i measured in bin j written as

$$P(E_j|C_i) = \frac{N_{ji}}{C_i},$$

where N_{ji} is the number of true events in bin i measured in bin j . 27

Iterative D'Agostini unfolding (2)

$P_{eff}(E_j | C_i)$ is defined as:

$$P_{eff}(E_j | C_i) = \frac{\frac{N_{ji}}{c_i}}{\sum_{i=1}^{N_m} \frac{N_{ji}}{c_i}},$$

where N_m is number of measured bins.

$P_0(C_i)$ is a prior probability representing the number of events in bin i , written as

$$P_0(C_i) = \frac{c_i}{\sum_{i=1}^{N_t} c_i}.$$

Therefore, the unfolded spectrum is

$$C'_i = \sum_{j=1}^{N_m} U_{ij} E_j^{\text{data}},$$

where N_m is the number of bins of measured spectrum.